








Capturing transient core-to-core resonances in Kr in intense extreme-ultraviolet laser fields by electron-ion coincidence spectroscopy

Mizuho Fushitani ^{1,2,*}, Makoto Yamada,¹ Hikaru Fujise,¹ Shigeki Owada ^{2,3}, Tadashi Togashi ^{2,3}, Kyo Nakajima ^{2,3}, Makina Yabashi,^{2,3} Akitaka Matsuda ^{1,2}, Yasumasa Hikosaka ^{4,2,†} and Akiyoshi Hishikawa ^{1,2,5,‡}

¹*Department of Chemistry, Graduate School of Science, Nagoya University, Nagoya, Aichi 464-8602, Japan*

²*RIKEN, SPring-8 Center, Sayo, Hyogo 679-5148, Japan*

³*Japan Synchrotron Radiation Research Institute, Sayo, Hyogo 679-5198, Japan*

⁴*Institute of Liberal Arts and Sciences, University of Toyama, Toyama 930-0194, Japan*

⁵*Research Center for Materials Science, Nagoya University, Nagoya, Aichi 464-8602, Japan*



(Received 12 October 2022; accepted 9 February 2023; published 23 February 2023)

Resonances between core-hole states have been long hypothesized to understand nonlinear responses of atoms and molecules exposed to intense x-ray free-electron laser (XFEL) pulses, but evaded clear identification in previous studies due to their transient nature. Here we report clear evidence of core-to-core resonances by state-of-the-art electron-ion coincidence spectroscopy on Kr atoms. The observed $3p$ - $3d$ resonance manifested the significance in multiple ionization to highly charged states against the ultrafast core-hole decay. The present study, elucidating the role of the core-to-core resonance in electronic responses of matter to high-frequency laser fields, will advance our understanding of nonlinear spectroscopy and ultrafast imaging by ultrashort intense EUV and x-ray pulses.

DOI: [10.1103/PhysRevA.107.L021101](https://doi.org/10.1103/PhysRevA.107.L021101)

Resonances are of great importance in light-matter interaction in strong laser fields, which enhance particular nonlinear processes by orders of magnitude. In extreme ultraviolet (EUV) and x-ray laser fields, the nonlinear responses of matter can be characterized by the participation of inner-shell or core electrons (see, for example, Refs. [1–5]), which makes a marked contrast to those in the visible and infrared regions. It was shown that the resonant excitation of core electrons into densely spaced Rydberg and valence states can enhance nonlinear photoionization to unexpectedly high charge states, as demonstrated with Ne [6,7], Kr [8], Xe [9,10], and CH_3I [11]. Resonances involving core electrons can be further enhanced by harnessing vacancies created in fully occupied orbitals during the interaction with the laser fields. Such resonance was identified with Ne [6], where ionization from the $1s$ core orbital is enhanced by $1s \rightarrow 2p$ resonance in singly ionized Ne at $h\nu = 848$ eV. Since the transition is not open in the neutral ground state, the resonance is often referred to as “hidden” resonances [6,12]. It is suggested that such resonances also play a decisive role in ultrafast diffraction imaging of nanoscale and biological systems using x-ray free-electron lasers (FELs) [13].

In addition to the core-to-valence resonances mentioned above, transient resonances can also occur between core-hole states, which have been indeed hypothesized to interpret the charge distribution of rare gas atoms, such as Kr and Xe [14] as well as Ar [15], exposed to intense x-ray pulses. The

core-to-core resonance has also been discussed in our previous study [16] of two-photon ionization to $4d$ double core-hole states of Xe, $\text{Xe} \xrightarrow{h\nu} \text{Xe}^+(4d^{-1}) + e^- \xrightarrow{h\nu} \text{Xe}^{2+}(4d^{-2}) + 2e^-$. The photoionization cross section of $\text{Xe}^+(4d^{-1})$ to $\text{Xe}^{2+}(4d^{-2})$ was found to be up to three times larger than the typical cross section of $4d$ inner-shell ionization [17,18], indicating an additional contribution to the well-known $4d$ giant resonance. To explain this unexpectedly large cross section, core-to-core resonant transitions from $4d^{-1}$ to $4p^{-1}$ states in Xe^+ were proposed because the $4p^{-1}$ states couple strongly with $4d^{-2}$ states. However, the broad spectral feature of the $4p^{-1}$ state spreading over 30 eV near the $4d^{-2}$ ionization threshold [19,20] prevented the unambiguous identification of resonances. Therefore, core-to-core resonant transitions have yet to be verified to fully understand the complex responses of matter in intense EUV and x-ray laser fields. Obviously, such resonances, hidden in neutral species in their ground states, require a transient core vacancy. The competition with core-hole decay proceeding in an ultrashort timescale ($\lesssim 10$ fs) makes the observation of the transient resonances challenging.

Here we present clear identification of hidden core-to-core transitions with Kr in intense EUV-FEL fields by using electron-ion coincidence spectroscopy [16,21]. In contrast to the strongly perturbed $\text{Xe}^+(4p^{-1})$ case, the $3p$ and $3d$ core-hole states of Kr are well defined in energy [22,23]. The optical transitions between the spin-orbit sublevels ($3p_{1/2,3/2}$ and $3d_{3/2,5/2}$) should appear with three distinct spectral lines around $h\nu = 120$ eV, which allows us to identify the $3p - 3d$ resonances as a function of the central photon energy of EUV-FEL. The $3p$ core-hole state formed in Kr^+ is detected by the $3p$ Auger electrons [24–26]. The coincidence electron

*fushitani@chem.nagoya-u.ac.jp

†hikosaka@las.u-toyama.ac.jp

‡hishi@chem.nagoya-u.ac.jp

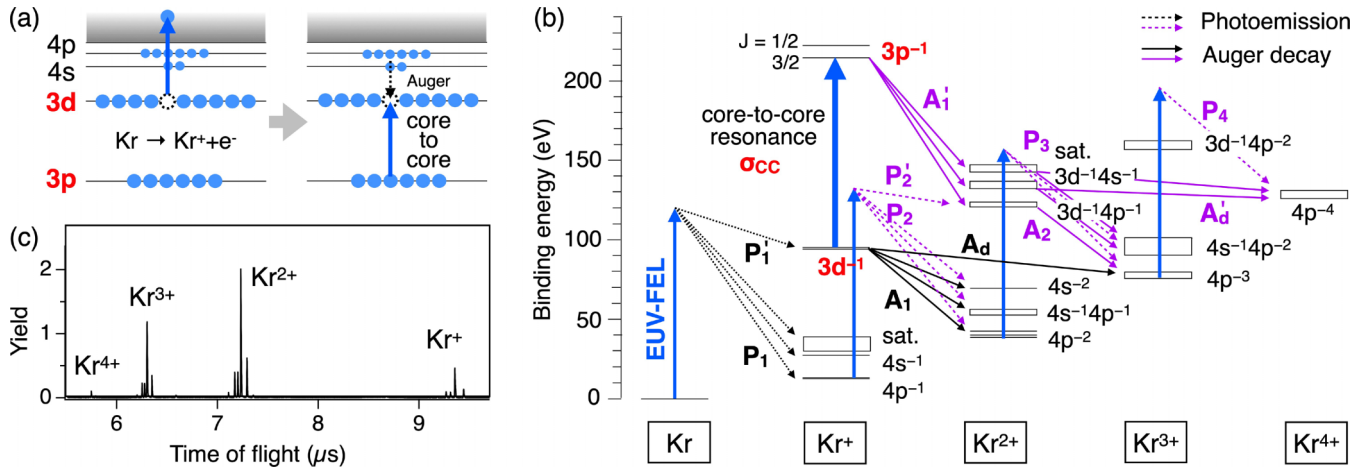


FIG. 1. (a) Schematic of transient core-to-core resonance at the $3p^{-1} - 3d^{-1}$ transition in the two-photon ionization of Kr, competing with ultrafast $3d$ core-hole decay. (b) Energy level diagram of Kr^{z+} ($z = 0-4$) [24,26–28] relevant to the present study. Possible multiple ionization pathways are shown by arrows representing photoabsorption and electron emission (black: single-photon process; purple: multiphoton process). (c) Time-of-flight spectrum of Kr in intense EUV-FEL laser fields (121.5 eV, 1.2×10^{14} W/cm²).

spectroscopy with the counterpart Kr^{3+} and Kr^{4+} ions, the major products via $3p$ core-hole decay [26] [see Fig. 1(b)], securely identifies the formation of the $3p$ core hole and the dependence of the FEL photon energy with minimal contamination from strong single-photon processes.

The experiments were conducted at the soft x-ray beam line (BL1) of SACLA [29]. Intense ultrashort EUV laser pulses ($h\nu = 118-128$ eV, bandwidth $\sim 1-2$ eV, pulse duration ~ 30 fs, repetition rate 60 Hz) [29,30] were focused by Kirkpatrick-Baez (KB) mirrors to gaseous Kr. Electrons and ions produced by the interaction with intense EUV pulses were detected by using a magnetic-bottle multielectron-ion coincidence spectrometer [16,21]. Briefly, the electrons are guided by a magnetic field toward a multichannel plate (MCP) detector placed at the end of the time-of-flight tube [31,32]. The counterpart ions were then collected by pulsed voltages applied approximately $1 \mu\text{s}$ after the laser irradiation to repeller (+4.0 kV) and extractor (+3.1 kV) electrodes, to be detected by the same MCP detector. In coincidence measurements, the sample pressure was kept at $\sim 4 \times 10^{-8}$ Pa. A Zr filter (0.1 μm) was used to suppress the harmonics of the FEL. The average event rate was 0.32 per laser shot. The typical energy resolution ΔE of the spectrometer can be given as $E/\Delta E = 33$ at the electron energy $E \lesssim 200$ eV. Electrons were decelerated by retarding electrodes to observe Kr $3p$ Auger peaks [24–26] with a high-energy resolution.

Figure 1(c) presents the ion time-of-flight mass spectrum of Kr in intense EUV-FEL fields (1.2×10^{14} W/cm²). The photon energy was tuned at 121.5 eV near the resonance (120.7 eV) expected from the difference between the $3p_{3/2}^{-1}$ and $3d_{5/2}^{-1}$ states [22]. Multiply charged Kr^{z+} ions up to $z = 4$ were observed in the spectrum. The lower charged ions ($z = 1-3$) were mainly produced by one-photon ionization to the $3d$ core-hole states followed by the Auger decay, while the formation of Kr^{4+} needs absorption of at least two photons. The electron spectrum recorded at a field intensity of 5.5×10^{14} W/cm² is shown in Fig. 2, which exhibits distinct peaks

at 108 and 93 eV corresponding to photoionization (P_1) to the $4p^{-1}$, $4s^{-1}$ and satellite states of Kr^+ [33,34] [see Fig. 1(b)]. Furthermore, the spectrum reveals an additional shoulderlike component at 92 eV and weak broad features below 100 eV, both of which become suppressed in the spectrum recorded at a lower laser field intensity (1.9×10^{13} W/cm²).

To understand how the peaks in the electron spectra that are nonlinearly proportional to the FEL intensity are correlated with the formation of Kr^{z+} ions ($z = 1-4$), the electron-ion coincidence events are collected and processed further by covariance analysis [35–37] to suppress the contributions from false coincidence events. The electron-ion covariance may be expressed as $\text{Cov}(X, Y) = \langle (X - \langle X \rangle)(Y - \langle Y \rangle) \rangle = \langle XY \rangle - \langle X \rangle \langle Y \rangle$, where X and Y are electron and ion signals, respectively, and the bracket denotes an average per laser shot. The second term corresponds to the contributions from false events, which is not negligible in the measurements recorded at the present event rate. Figure 3(a) shows the electron spectrum correlated with Kr^+ , exhibiting the peaks (P_1) associated with valence ionization of Kr. These peaks also

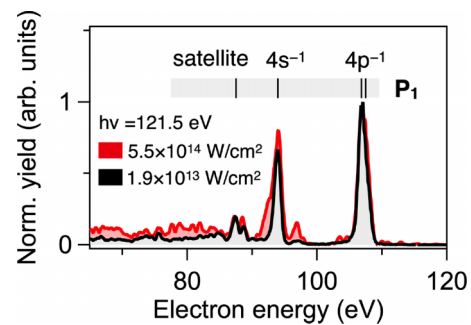


FIG. 2. Total electron spectra of Kr at $h\nu = 121.5$ eV, recorded with a retarding voltage of -57 V. The laser field intensities of 1.9×10^{13} W/cm² (gray) and 5.5×10^{14} W/cm² (red). Sticks represent energies of photoelectrons (P_1) to the $4p^{-1}$, $4s^{-1}$ and satellite states of Kr^+ . The spectra are normalized at the $4p$ photoelectron peak.

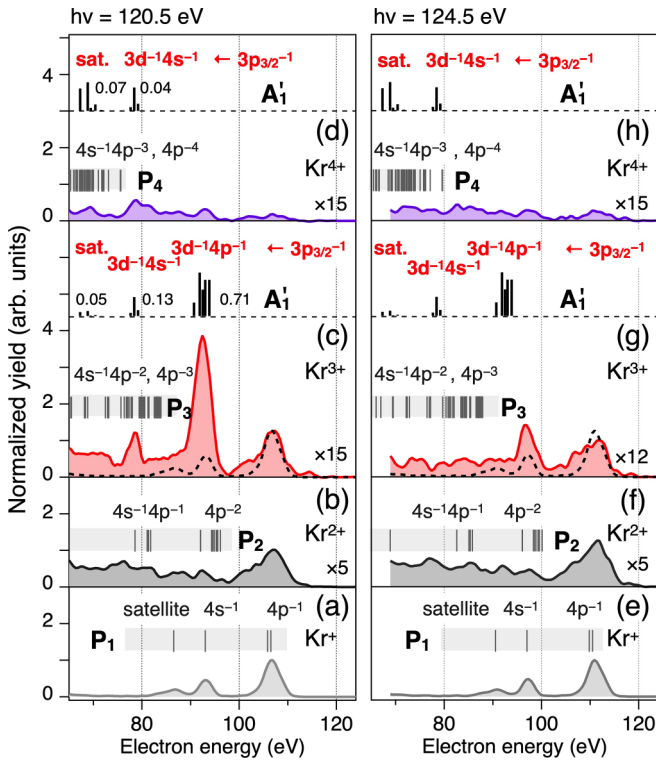


FIG. 3. Electron spectra recorded in coincidence with (a) Kr^+ , (b) Kr^{2+} , (c) Kr^{3+} , and (d) Kr^{4+} ions, respectively, at $h\nu = 120.5$ eV (1.2×10^{14} W/cm 2). Thin sticks represent the electron energies expected for valence photoionization [P_1 , P_2 , P_3 , and P_4 , in Fig. 1(b)]. Thick stick spectra stand for the $3p_{3/2}$ Auger peaks (A_1') with the relative intensities [25,26]. The dotted curve in (c) is the same one in (a), showing that there is a contribution in the Kr^{3+} yield from a sequential two-photon ionization pathway through the Kr^+ valence states in addition to a two-photon pathway via the Kr^+ $3p_{3/2}^{-1}$ state. (e)–(h) Same as (a)–(d), but for $h\nu = 124.5$ eV.

appear in Fig. 3(b) for Kr^{2+} , showing that Kr^{2+} can be formed via the Kr^+ states. The features appearing at 65–100 eV are attributed to photoelectrons (P_2) produced by photoionization of the Kr^+ $4p^{-1}$ states to the $4s^{-1}4p^{-1}$ and $4p^{-2}$ states of Kr^{2+} , as well as those from $4s^{-1}$ to $4s^{-1}4p^{-1}$ [thin stick spectra in Fig. 3(b)]. In addition, photoionization from Kr^+ satellite states, such as Kr^+ ($4p^{-1}4s^{-1}nl$) + $h\nu \rightarrow \text{Kr}^{2+}$ ($4p^{-2}4s^{-1}n'l'$) + e^- , appears in this energy region. Because of the contributions from these electronic states, a quasicontinuum distribution is formed in the photoelectron spectrum. The broad distribution below ~ 80 eV may also be attributed to one-photon double ionization of Kr, where two $4p$ photoelectrons share the extra energy of 81.7 eV above the double-ionization threshold (38.8 eV [27]).

The electron spectrum recorded with Kr^{3+} in Fig. 3(c) exhibits a prominent peak at 92.4 eV, with an additional peak at 78.4 eV. The former corresponds to the shoulderlike component observed in Fig. 2. The observed electron energies are in good agreement with those reported for the Auger decay (A_1') from the $3p_{3/2}^{-1}$ core-hole state to the $3d^{-1}4p^{-1}$ and $3d^{-1}4s^{-1}$ states [24–26]. In addition, the relative intensities agree well with those expected for the $3p_{3/2}^{-1}$ Auger decay [thick stick spectra in Fig. 3(c)], where the branching to the Kr^{3+} and

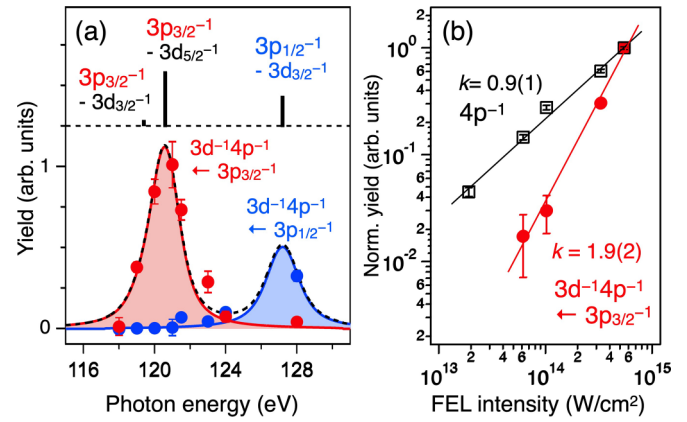


FIG. 4. (a) Auger electron yields from the Kr^+ core-hole states, $3p_{3/2}^{-1}$ (red) and $3p_{1/2}^{-1}$ (blue), decaying to Kr^{2+} ($3d^{-1}4p^{-1}$), as a function of the FEL photon energy. Expected transition energies [22], $h\nu = 127.3$ eV ($3p_{1/2}^{-1} - 3d_{5/2}^{-1}$), 120.7 eV ($3p_{3/2}^{-1} - 3d_{5/2}^{-1}$), and 119.5 eV ($3p_{3/2}^{-1} - 3d_{3/2}^{-1}$), are shown in the upper panel, together with the line strengths estimated from the statistical weights in the Russell-Saunders coupling scheme [39]. The stick spectra convoluted with the FEL width (1.1 eV) as well as the natural line widths of the $3p_{3/2}^{-1}$ (1.28 eV) and $3p_{1/2}^{-1}$ (1.65 eV) states [24] are also shown (solid lines) to compare with the experimental results. (b) FEL field-intensity dependence of the $4p$ photoelectron yield (open square) and $3p_{3/2}^{-1}$ Auger electron yield to the $3d^{-1}4p^{-1}$ state (solid circle). Results of the least-squares fitting to a power function I^k are also shown.

Kr^{4+} final states [25,26] is taken into account. Note that the peak at 92.4 eV is hardly seen in the Kr^{4+} spectrum [Fig. 3(d)] because the dominant intermediate states, Kr^{2+} $3d^{-1}4p^{-1}$, are located below the $4p^{-4}$ ground state of Kr^{4+} [see Fig. 1(b)].

Figures 3(e)–3(h) show the corresponding spectra recorded at a different photon energy of $h\nu = 124.5$ eV, where all of the $3p$ Auger peaks become suppressed. This photon-energy dependence suggests a resonance contribution to produce the $3p^{-1}$ core hole, depicted in Fig. 1(a). To securely confirm the core-to-core resonance from the $3d^{-1}$ to $3p^{-1}$ states, the Auger peak intensity at 92.4 eV from the $3p_{3/2}^{-1}$ core hole is estimated from the total electron spectra as a function of the FEL photon energy (see Supplemental Material [38]). As shown in Fig. 4(a), the $3p_{3/2}^{-1}$ Auger signal exhibits a peak around $h\nu = 121$ eV, which agrees well with the energy difference between the $3p_{3/2}^{-1}$ and $3d_{5/2}^{-1}$ states calculated from their state energies [22].

The observed spectrum is well reproduced by stick spectra for the $3p_{3/2}^{-1} - 3d_{5/2}^{-1}$ and $3p_{3/2}^{-1} - 3d_{3/2}^{-1}$ transitions, where the line strengths are calculated by the statistical weights of each state. The stick spectra are convoluted with the natural widths of the $3p_{3/2}^{-1}$ (1.28 eV) and $3p_{1/2}^{-1}$ (1.65 eV) states [24] and the FEL spectral width (1.1 eV), which explains the observed photon-energy dependence, as shown in Fig. 4(a). Figure 4(a) also shows that the Auger electron from the upper spin-orbit component $3p_{1/2}^{-1}$ appears at higher photon energies $h\nu = 128$ eV, which is consistent with the core-to-core resonance transition between the $3p_{1/2}^{-1}$ and $3d_{3/2}^{-1}$ core-hole states.

Figure 4(b) plots the integrated intensity of the $3p_{3/2}^{-1} \rightarrow 3d^{-1}4p^{-1}$ Auger peak as a function of FEL field intensity

I at $h\nu = 120.5$ eV. The field-intensity dependence is well expressed by I^k with $k = 1.9$ (2), supporting that the $3p_{3/2}^{-1}$ core hole is produced by two-photon processes, filling the vacant $3d$ orbital by an electron from the deeper-lying $3p$ orbital.

It is worth noting that the electron spectrum for Kr^{3+} in Fig. 3(c) shows features from the P_1 and P_3 photoelectrons, in addition to the Auger electrons from the $3p^{-1}$ state (A'_1) discussed above. This indicates that the photoionization to Kr^{3+} also proceeds from the $\text{Kr}^+ 4l^{-1}$ and $\text{Kr}^{2+} 4l^{-1}4l'^{-1}$ states [see Fig. 1(b)]. The quantitative contributions to the electron spectrum can be estimated from the integrated intensities of the corresponding spectra (see Supplemental Material [38]). Briefly, the net signals from the core-to-core transition, $S(3p_{3/2}^{-1})$, in Fig. 3(c) are obtained by subtraction of a scaled off-resonance spectrum in Fig. 3(g). The relative contribution $S(4l^{-1})$ from the $4l^{-1}$ pathway is obtained as the integrated intensity of the P_1 photoelectron spectrum in Fig. 3(e) normalized at the $4p^{-1}$ peak of the off-resonance spectrum. The ratio between the core and the $4l^{-1}$ valence pathways is obtained as $S(3p_{3/2}^{-1})/S(4l^{-1}) = 1.4(2)$. These show that the $3p^{-1} - 3d^{-1}$ core-to-core resonant transition efficiently takes place under the present experimental conditions even though the lifetime of the intermediate $3d$ core-hole state (7.4 fs [40]) is substantially shorter than the FEL pulse duration (28 fs [30]).

For a more quantitative discussion, numerical simulations solving coupled rate equations for multiphoton ionization of Kr [Fig. 1(b)] were carried out (see Supplemental Material [38]). For simplicity, cross sections of the valence and the $3d$ photoionization of Kr^+ and Kr^{2+} are assumed to be the same as those for Kr, 0.37 Mb and 2.54 Mb, respectively [41,42]. In addition, the lifetime of $3d$ core-hole states of Kr^{2+} was set to that of Kr^+ (7.4 fs [40]), while the $3p_{3/2}^{-1}$ core hole, having an ultrashort lifetime (0.6 fs [24]), was assumed to instantaneously decay to the $3d^{-1}4p^{-1}$, $3d^{-1}4s^{-1}$, and satellite states. The photoabsorption cross section of the $3p^{-1} - 3d^{-1}$ core-to-core transition, σ_{CC} , was treated as an adjustable parameter in the simulation. It was found that the observed yield ratio $S(3p_{3/2}^{-1})/S(4l^{-1})$ is reproduced with $\sigma_{\text{CC}}(3p_{3/2}^{-1} - 3d_{5/2}^{-1}) = 1.6 \pm 0.2$ Mb. The obtained value may be compared with cross sections of dipole-allowed transitions of Kr [43], for instance, the excitation cross section to the $3p^{-1}4d$ state, $\sigma \sim 0.3$ Mb, estimated from a photoabsorption spectrum [44].

Figure 5(a) plots the yields of the Kr^{z+} ions ($z = 1-4$) recorded as a function of the FEL field intensity ($h\nu = 120.5$ eV). As the FEL intensity increases, the yields of the lower charged states ($z = 1-3$) become saturated at $\sim 5 \times 10^{14}$ W/cm², as they are mainly produced by the one-photon $3d$ ionization [Fig. 1(b)]. On the other hand, a steep increase is observed for Kr^{4+} that requires absorption of more than one photon for the production. These behaviors are well reproduced by the curves simulated with the cross section $\sigma_{\text{CC}}(3p_{3/2}^{-1} - 3d_{5/2}^{-1})$ determined above. Figures 5(b) and 5(c) show the contributions from individual pathways leading to Kr^{3+} and Kr^{4+} , respectively. At low intensities below 10^{14} W/cm², Kr^{3+} is essentially produced by one-photon $3d$ ionization as discussed above, while the contribution from the pathway via the $3p^{-1}$ core-hole state becomes significant at

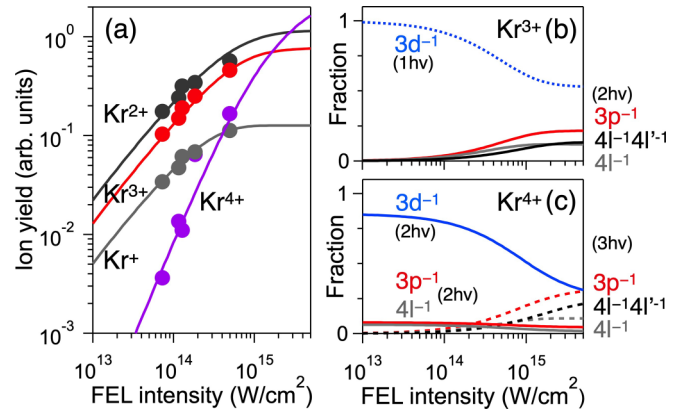


FIG. 5. (a) Total yields of Kr^+ (gray), Kr^{2+} (black), Kr^{3+} (red), and Kr^{4+} (yellow) ions as a function of FEL intensity. Results of the simulation are obtained with $\sigma_{\text{CC}} = 1.6$ Mb (solid lines). (b) Simulated relative yields in multiple ionization to Kr^{3+} from one-photon pathways (dotted line): (i) via $\text{Kr}^+(3d^{-1})$ with an electron emission sequence of $P'_1 - A_d$ and from two-photon pathway (solid line): (ii) via $\text{Kr}^+(4l^{-1})$ with $P_1 - P'_2 - A_2$ and (iii) via $\text{Kr}^{2+}(4l^{-1}4l'^{-1})$ with $P'_1 - A_1 - P_3$ [see Fig. 1(b)]. (c) Same as (b), but for Kr^{4+} . Results of three two-photon pathways are shown (solid): (i) via $\text{Kr}^+(3d^{-1})$ with $P'_1 - A_d - P_4$ (blue), (ii) via $\text{Kr}^+(3p^{-1})$ with $P'_1 - A'_1 - A'_d$ (red), and (iii) via $\text{Kr}^+(4l^{-1})$ with $P_1 - P'_2 - A'_d$ (gray). Three-photon pathways (dashed lines) are shown for those (i) via $\text{Kr}^+(4l^{-1})$ with $P_1 - P'_2 - A_2 - P_4$, (ii) via $\text{Kr}^{2+}(4l^{-1}4l'^{-1})$ with $P'_1 - A_1 - P_3 - P_4$, and (iii) via $\text{Kr}^+(3p^{-1})$ with $P'_1 - A'_1 - A_2 - P_4$.

higher field intensities. For Kr^{4+} , the two-photon pathway via the double Auger decay from the $3d^{-1}$ states is dominant at the low field intensities. The three-photon pathway via $3p^{-1}$ (see Fig. 1) becomes one of the major pathways at 5×10^{15} W/cm², showing that the effect of core-to-core resonance becomes significant at high field intensities against the ultrafast Auger decay of the intermediate $3d$ core-hole state.

In summary, we captured transient resonances between core-hole states during multiple ionization of Kr in intense EUV-FEL fields by electron-ion coincidence spectroscopy. The resonance between the core-hole states, which eluded clear identification in previous studies, is observed between $3p^{-1}$ and $3d^{-1}$ states of Kr at $h\nu = 121$ eV, which manifested the significance in the multiple ionization to highly charged Kr^{z+} ($z = 3, 4$). Nonlinear responses of matter to high-frequency laser fields are inherently complex, as photoabsorption proceeds along various pathways consisting of different sequences with competing Auger and radiative processes. As has been discussed in the previous study [14–16], transient core-to-core resonance is not specific to Kr and is expected to be common in other targets. The present study shows that the core-to-core resonance is a crucial ingredient to understand the complicated nature of the nonlinear responses of matter, ranging from isolated molecules [11,45] to bulk materials [46], in intense EUV and x-ray laser fields, in particular generated by broadband FEL pulses covering a wide photon-energy range for resonance transitions [14].

Recently, the methodology of quantum control has been extended to high-frequency regions [47–49]. In this regard,

this study demonstrating the feasibility of core-to-core excitation against ultrafast core-hole decay presents a significant step toward coherent control of transferring an electron hole between inner-shell levels. The quantum control on core-hole states by EUV and x-ray laser pulses will allow us to actively manipulate local atomic states within a molecule, rather than the valence and Rydberg states that spread over the molecule, thus offering new approaches for element-specific chemical analysis and control of processes involving core-hole states such as intermolecular Coulombic decay [50].

We are grateful to the operation and engineering staff members of SACLA, Shunya Koizumi and Naoto Taguchi (Nagoya University), for their assistance during the beam time. This work is supported by JSPS KAKENHI (Grants No. JP18K03489, No. JP20K05549, No. JP21K03430), Integrated Research Consortium on Chemical Sciences (IRCCS) and World Research Unit (B-1) of Reaction Infography (R-ing) at Nagoya University. This research was carried out at SACLA BL1 with the approval of the Japan Synchrotron Radiation Research Institute (JASRI) (Proposals No. 2019B8046, No. 2021A8052, No. 2021B8072).

-
- [1] E. A. Seddon, J. A. Clarke, D. J. Dunning, C. Masciovecchio, C. J. Milne, F. Parmigiani, D. Rugg, J. C. Spence, N. R. Thompson, K. Ueda, S. M. Vinko, J. S. Wark, and W. Wurth, Short-wavelength free-electron laser sources and science: A review, *Rep. Prog. Phys.* **80**, 115901 (2017).
- [2] H. Fukuzawa and K. Ueda, X-ray induced ultrafast dynamics in atoms, molecules, and clusters: Experimental studies at an x-ray free-electron laser facility SACLA and modeling, *Adv. Phys.: X* **5**, 1785327 (2020).
- [3] M. Yabashi, H. Tanaka, T. Tanaka, H. Tomizawa, T. Togashi, M. Nagasono, T. Ishikawa, J. R. Harries, Y. Hikosaka, A. Hishikawa, K. Nagaya, N. Saito, E. Shigemasa, K. Yamanouchi, and K. Ueda, Compact XFEL and AMO sciences: SACLA and SCSS, *J. Phys. B: At. Mol. Opt. Phys.* **46**, 164001 (2013).
- [4] J. Feldhaus, M. Krikunova, M. Meyer, T. Möller, R. Moshhammer, A. Rudenko, T. Tschentscher, and J. Ullrich, AMO science at the FLASH and European XFEL free-electron laser facilities, *J. Phys. B: At. Mol. Opt. Phys.* **46**, 164002 (2013).
- [5] C. Bostedt, J. D. Bozek, P. H. Bucksbaum, R. N. Coffee, J. B. Hastings, Z. Huang, R. W. Lee, S. Schorb, J. N. Corlett, P. Denes, P. Emma, R. W. Falcone, R. W. Schoenlein, G. Doumy, E. P. Kanter, B. Kraessig, S. Southworth, L. Young, L. Fang, M. Hoener *et al.*, Ultra-fast and ultra-intense x-ray sciences: First results from the Linac Coherent Light Source free-electron laser, *J. Phys. B: At. Mol. Opt. Phys.* **46**, 164003 (2013).
- [6] E. P. Kanter, B. Krässig, Y. Li, A. M. March, P. Ho, N. Rohringer, R. Santra, S. H. Southworth, L. F. DiMauro, G. Doumy, C. A. Roedig, N. Berrah, L. Fang, M. Hoener, P. H. Bucksbaum, S. Ghimire, D. A. Reis, J. D. Bozek, C. Bostedt, M. Messerschmidt *et al.*, Unveiling and Driving Hidden Resonances with High-Fluence, High-Intensity X-Ray Pulses, *Phys. Rev. Lett.* **107**, 233001 (2011).
- [7] T. Mazza, M. Ilchen, M. D. Kiselev, E. V. Gryzlova, T. M. Baumann, R. Boll, A. De Fanis, P. Grychtol, J. Montano, V. Music, Y. Ovcharenko, N. Rennhack, D. E. Rivas, P. Schmidt, R. Wagner, P. Ziolkowski, N. Berrah, B. Erk, P. Johnsson, C. Küstner-Wetekam *et al.*, Mapping Resonance Structures in Transient Core-Ionized Atoms, *Phys. Rev. X* **10**, 041056 (2020).
- [8] B. Rudek, D. Rolles, S. K. Son, L. Foucar, B. Erk, S. Epp, R. Boll, D. Anielski, C. Bostedt, S. Schorb, R. Coffee, J. Bozek, S. Trippel, T. Marchenko, M. Simon, L. Christensen, S. De, S. I. Wada, K. Ueda, I. Schlichting *et al.*, Resonance-enhanced multiple ionization of krypton at an x-ray free-electron laser, *Phys. Rev. A* **87**, 023413 (2013).
- [9] B. Rudek, S. K. Son, L. Foucar, S. W. Epp, B. Erk, R. Hartmann, M. Adolph, R. Andritschke, A. Aquila, N. Berrah, C. Bostedt, J. Bozek, N. Coppola, F. Filsinger, H. Gorke, T. Gorkhover, H. Graafsma, L. Gumprecht, A. Hartmann, G. Hauser *et al.*, Ultra-efficient ionization of heavy atoms by intense x-ray free-electron laser pulses, *Nat. Photon.* **6**, 858 (2012).
- [10] B. Rudek, K. Toyota, L. Foucar, B. Erk, R. Boll, C. Bomme, J. Correa, S. Carron, S. Boutet, G. J. Williams, K. R. Ferguson, R. Alonso-Mori, J. E. Koglin, T. Gorkhover, M. Bucher, C. S. Lehmann, B. Krässig, S. H. Southworth, L. Young, C. Bostedt *et al.*, Relativistic and resonant effects in the ionization of heavy atoms by ultra-intense hard x-rays, *Nat. Commun.* **9**, 4200 (2018).
- [11] X. Li, A. Rudenko, T. Mazza, A. Rörig, N. Anders, T. M. Baumann, S. Eckart, B. Erk, A. De Fanis, K. Fehre, R. Dörner, L. Foucar, S. Grundmann, P. Grychtol, A. Hartung, M. Hofmann, M. Ilchen, C. Janke, G. Kastirke, M. Kircher *et al.*, Resonance-enhanced x-ray multiple ionization of a polyatomic molecule, *Phys. Rev. A* **105**, 053102 (2022).
- [12] P. J. Ho, C. Bostedt, S. Schorb, and L. Young, Theoretical Tracking of Resonance-Enhanced Multiple Ionization Pathways in X-ray Free-Electron Laser Pulses, *Phys. Rev. Lett.* **113**, 253001 (2014).
- [13] P. J. Ho, B. J. Daurer, M. F. Hantke, J. Bielecki, A. Al Haddad, M. Bucher, G. Doumy, K. R. Ferguson, L. Flückiger, T. Gorkhover, B. Iwan, C. Knight, S. Moeller, T. Osipov, D. Ray, S. H. Southworth, M. Svenda, N. Timneanu, A. Ulmer, P. Walter *et al.*, The role of transient resonances for ultra-fast imaging of single sucrose nanoclusters, *Nat. Commun.* **11**, 167 (2020).
- [14] P. J. Ho, E. P. Kanter, and L. Young, Resonance-mediated atomic ionization dynamics induced by ultraintense x-ray pulses, *Phys. Rev. A* **92**, 063430 (2015).
- [15] A. C. LaForge, S. K. Son, D. Mishra, M. Ilchen, S. Duncanson, E. Eronen, E. Kukk, S. Wirok-Stoletow, D. Kolbasova, P. Walter, R. Boll, A. De Fanis, M. Meyer, Y. Ovcharenko, D. E. Rivas, P. Schmidt, S. Usenko, R. Santra, and N. Berrah, Resonance-Enhanced Multiphoton Ionization in the X-Ray Regime, *Phys. Rev. Lett.* **127**, 213202 (2021).
- [16] M. Fushitani, Y. Sasaki, A. Matsuda, H. Fujise, Y. Kawabe, K. Hashigaya, S. Owada, T. Togashi, K. Nakajima, M. Yabashi, Y. Hikosaka, and A. Hishikawa, Multielectron-Ion Coincidence Spectroscopy of Xe in Extreme Ultraviolet Laser Fields:

- Nonlinear Multiple Ionization via Double Core-Hole States, *Phys. Rev. Lett.* **124**, 193201 (2020).
- [17] U. Becker, D. Szostak, H. G. Kerkhoff, M. Kupsch, B. Langer, R. Wehlitz, A. Yagishita, and T. Hayaishi, Subshell photoionization of Xe between 40 and 1000 eV, *Phys. Rev. A* **39**, 3902 (1989).
- [18] P. Andersen, T. Andersen, F. Folkmann, V. K. Ivanov, H. Kjeldsen, and J. B. West, Absolute cross sections for the photoionization of $4d$ electrons in Xe^+ and Xe^{2+} ions, *J. Phys. B: At. Mol. Opt. Phys.* **34**, 2009 (2001).
- [19] G. Wendin and M. Ohno, Strong dynamical effects of many-electron interactions in photoelectron spectra from $4s$ and $4p$ core levels, *Phys. Scr.* **14**, 148 (1976).
- [20] S. Svensson, N. Mårtensson, E. Basilier, P. Malmquist, U. Gelius, and K. Siegbahn, Lifetime broadening and CI-resonances observed in ESCA, *Phys. Scr.* **14**, 141 (1976).
- [21] A. Matsuda, M. Fushitani, C. M. Tseng, Y. Hikosaka, J. H. Eland, and A. Hishikawa, A magnetic-bottle multi-electron-ion coincidence spectrometer, *Rev. Sci. Instrum.* **82**, 103105 (2011).
- [22] K. Siegbahn, C. Nordling, G. Johansson, J. Hedman, P. F. Hedén, K. Hamrin, U. Gelius, T. Bergmark, L. O. Werme, R. Manne, and Y. Baer, *ESCA Applied to Free Molecules* (North-Holland, Amsterdam, 1969).
- [23] S. Kosugi, F. Koike, T. Nagayasu, F. Hosseini, J. Martins, T. Marchenko, O. Travnikova, M. Oura, T. Gejo, J. R. Harries, J. D. Bozek, K. Ito, E. Sokell, S. Fritzsche, M. N. Piancastelli, M. Simon, and Y. Azuma, Strong configuration interaction in the $3p$ photoelectron spectrum of Kr, *Phys. Rev. A* **101**, 042505 (2020).
- [24] J. Jauhiainen, A. Kivimäki, S. Aksela, O. P. Sairanen, and H. Aksela, Auger and Coster-Kronig decay of the $3p$ hole states in krypton, *J. Phys. B: At. Mol. Opt. Phys.* **28**, 4091 (1995).
- [25] Y. Hikosaka, P. Lablanquie, T. Kaneyasu, J. Adachi, H. Tanaka, I. H. Suzuki, M. Ishikawa, and T. Odagiri, Super-Coster-Kronig decay of Kr $3p$ core-hole states studied by multielectron coincidence spectroscopy, *Phys. Rev. A* **103**, 043119 (2021).
- [26] Y. Hikosaka, P. Lablanquie, T. Kaneyasu, J. Adachi, H. Tanaka, I. H. Suzuki, M. Ishikawa, and T. Odagiri, Auger cascade initiated by the Coster-Kronig transition from the Kr $3p$ core-hole states, *J. Phys. B: At. Mol. Opt. Phys.* **54**, 185002 (2021).
- [27] A. Kramida, Y. Ralchenko, J. Reader, and NIST ASD Team (2021), NIST Atomic Spectra Database (ver. 5.9), <https://physics.nist.gov/asd> (National Institute of Standards and Technology, Gaithersburg, MD, 2021).
- [28] V. Jonauskas, S. Kučas, and R. Karazija, Auger decay of $3p$ -ionized krypton, *Phys. Rev. A* **84**, 053415 (2011).
- [29] S. Owada, K. Togawa, T. Inagaki, T. Hara, T. Tanaka, Y. Joti, T. Koyama, K. Nakajima, H. Ohashi, Y. Senba, T. Togashi, K. Tono, M. Yamaga, H. Yumoto, M. Yabashi, H. Tanaka, and T. Ishikawa, A soft x-ray free-electron laser beam line at SACLA: The light source, photon beam line and experimental station, *J. Synchrotron Rad.* **25**, 282 (2018).
- [30] S. Owada, M. Fushitani, A. Matsuda, H. Fujise, Y. Sasaki, Y. Hikosaka, A. Hishikawa, and M. Yabashi, Characterization of soft x-ray FEL pulse duration with two-color photoelectron spectroscopy, *J. Synchrotron Rad.* **27**, 1362 (2020).
- [31] Y. Hikosaka, M. Fushitani, A. Matsuda, C. M. Tseng, A. Hishikawa, E. Shigemasa, M. Nagasono, K. Tono, T. Togashi, H. Ohashi, H. Kimura, Y. Senba, M. Yabashi, and T. Ishikawa, Multiphoton Double Ionization of Ar in Intense Extreme Ultraviolet Laser Fields Studied by Shot-by-Shot Photoelectron Spectroscopy, *Phys. Rev. Lett.* **105**, 133001 (2010).
- [32] A. Hishikawa, M. Fushitani, Y. Hikosaka, A. Matsuda, C. N. Liu, T. Morishita, E. Shigemasa, M. Nagasono, K. Tono, T. Togashi, H. Ohashi, H. Kimura, Y. Senba, M. Yabashi, and T. Ishikawa, Enhanced Nonlinear Double Excitation of He in Intense Extreme Ultraviolet Laser Fields, *Phys. Rev. Lett.* **107**, 243003 (2011).
- [33] S. Svensson, B. Eriksson, N. Mårtensson, G. Wendin, and U. Gelius, Electron shake-up and correlation satellites and continuum shake-off distributions in x-ray photoelectron spectra of the rare gas atoms, *J. Electron Spectrosc. Relat. Phenom.* **47**, 327 (1988).
- [34] A. Kikas, S. J. Osborne, A. Ausmees, S. Svensson, O. P. Sairanen, and S. Aksela, High-resolution study of the correlation satellites in photoelectron spectra of the rare gases, *J. Electron Spectrosc. Relat. Phenom.* **77**, 241 (1996).
- [35] L. J. Frasinski, V. Zhaunerchyk, M. Mucke, R. J. Squibb, M. Siano, J. H. D. Eland, P. Linusson, P. v. d. Meulen, P. Salen, R. D. Thomas, M. Larsson, L. Foucar, J. Ullrich, K. Motomura, S. Mondal, K. Ueda, T. Osipov, L. Fang, B. F. Murphy, N. Berrah *et al.*, Dynamics of Hollow Atom Formation in Intense X-Ray Pulses Probed by Partial Covariance Mapping, *Phys. Rev. Lett.* **111**, 073002 (2013).
- [36] V. Zhaunerchyk, L. J. Frasinski, J. H. D. Eland, and R. Feifel, Theory and simulations of covariance mapping in multiple dimensions for data analysis in high-event-rate experiments, *Phys. Rev. A* **89**, 053418 (2014).
- [37] F. Allum, N. Anders, M. Brouard, P. Bucksbaum, M. Burt, B. Downes-Ward, S. Grundmann, J. Harries, Y. Ishimura, H. Iwayama, L. Kaiser, E. Kukk, J. Lee, X. Liu, R. S. Minns, K. Nagaya, A. Niozu, J. Niskanen, J. O'Neal, S. Owada *et al.*, Multi-channel photodissociation and XUV-induced charge transfer dynamics in strong-field-ionized methyl iodide studied with time-resolved recoil-frame covariance imaging, *Faraday Discuss.* **228**, 571 (2021).
- [38] See Supplemental Material at <http://link.aps.org/supplemental/10.1103/PhysRevA.107.L021101> for details.
- [39] E. U. Condon and G. H. Shortley, *The Theory of Atomic Spectra* (Cambridge University Press, Cambridge, 1953).
- [40] M. Jurvansuu, A. Kivimäki, and S. Aksela, Inherent lifetime widths of Ar $2p^{-1}$, Kr $3d^{-1}$, Xe $3d^{-1}$ and Xe $4d^{-1}$ states, *Phys. Rev. A* **64**, 012502 (2001).
- [41] N. Saito and I. H. Suzuki, Multiple photoionization in Ne, Ar, Kr and Xe from 44 to 1300 eV, *Intl. J. Mass Spectrom. Ion Process.* **115**, 157 (1992).
- [42] M. Lu, G. Alna'washi, M. Habibi, M. F. Gharaibeh, R. A. Phaneuf, A. L. D. Kilcoyne, E. Levenson, A. S. Schlachter, C. Cisneros, and G. Hinojosa, Photoionization and electron-impact ionization of Kr^{3+} , *Phys. Rev. A* **74**, 062701 (2006).
- [43] W. F. Chan, G. Cooper, X. Guo, G. R. Burton, and C. E. Brion, Absolute optical oscillator strengths for the electronic excitation of atoms at high resolution. III. The photoabsorption of argon, krypton, and xenon, *Phys. Rev. A* **46**, 149 (1992).
- [44] R. Sankari, A. Kivimäki, H. Aksela, S. Aksela, K. C. Prince, M. Coreno, M. Alagia, and M. de Simone, Krypton $3p$ excitations and subsequent resonant Auger decay, *Phys. Rev. A* **67**, 032710 (2003).

- [45] A. Rudenko, L. Inhester, K. Hanasaki, X. Li, S. J. Robatjazi, B. Erk, R. Boll, K. Toyota, Y. Hao, O. Vendrell, C. Bomme, E. Savelyev, B. Rudek, L. Foucar, S. H. Southworth, C. S. Lehmann, B. Kraessig, T. Marchenko, M. Simon, K. Ueda *et al.*, Femtosecond response of polyatomic molecules to ultra-intense hard x-rays, *Nature (London)* **546**, 129 (2017).
- [46] I. Inoue, Y. Inubushi, T. Osaka, J. Yamada, K. Tamasaku, H. Yoneda, and M. Yabashi, Shortening X-Ray Pulse Duration via Saturable Absorption, *Phys. Rev. Lett.* **127**, 163903 (2021).
- [47] Y. Hikosaka, T. Kaneyasu, M. Fujimoto, H. Iwayama, and M. Katoh, Coherent control in the extreme ultraviolet and attosecond regime by synchrotron radiation, *Nat. Commun.* **10**, 4988 (2019).
- [48] A. Wituschek, L. Bruder, E. Allaria, U. Bangert, M. Binz, R. Borghes, C. Callegari, G. Cerullo, P. Cinquegrana, L. Giannessi, M. Danailov, A. Demidovich, M. Di Fraia, M. Drabbels, R. Feifel, T. Laarmann, R. Michiels, N. S. Mirian, M. Mudrich, I. Nikolov *et al.*, Tracking attosecond electronic coherences using phase-manipulated extreme ultraviolet pulses, *Nat. Commun.* **11**, 883 (2020).
- [49] S. Nandi, E. Olofsson, M. Bertolino, S. Carlström, F. Zapata, D. Busto, C. Callegari, M. Di Fraia, P. Eng-Johnsson, R. Feifel, G. Gallician, M. Gisselbrecht, S. Maclot, L. Neoričić, J. Peschel, O. Plekan, K. C. Prince, R. J. Squibb, S. Zhong, P. V. Demekhin *et al.*, Observation of Rabi dynamics with a short-wavelength free-electron laser, *Nature (London)* **608**, 488 (2022).
- [50] T. Jahnke, U. Hergenhahn, B. Winter, R. Dörner, U. Fröhling, P. V. Demekhin, K. Gokhberg, L. S. Cederbaum, A. Ehresmann, A. Knie, and A. Dreuw, Interatomic and intermolecular Coulombic decay, *Chem. Rev.* **120**, 11295 (2020).